Bioresource Technology 111 (2012) 433–438

Contents lists available at SciVerse ScienceDirect

Bioresource Technology

journal homepage: www.elsevier.com/locate/biortech

Torrefied biomasses in a drop tube furnace to evaluate their utility in blast furnaces

Wei-Hsin Chen [a],*, Shan-Wen Du [b], Chien-Hsiung Tsai [c], Zhen-Yu Wang [c]

[a] Department of Greenergy, National University of Tainan, Tainan 700, Taiwan, ROC
[b] Iron and Steel Research and Development Department, China Steel Corporation, Kaohsiung 812, Taiwan, ROC
[c] Department of Vehicle Engineering, National Pingtung University of Science and Technology, Pingtung, Taiwan, ROC

ARTICLE INFO

Article history:
Received 1 October 2011
Received in revised form 24 January 2012
Accepted 26 January 2012
Available online 14 February 2012

Keywords:
Torrefaction and pretreatment
Pulverized coal injection (PCI)
Drop tube furnace
Burnout
R-factor

ABSTRACT

Torrefaction and burning characteristics of bamboo, oil palm, rice husk, bagasse, and Madagascar almond were studied and compared with a high-volatile bituminous coal using a drop tube furnace to evaluate the potential of biomass consumed in blast furnaces. Torrefaction at 250 and 300 °C for 1 h duration was carried out. Analysis using the ash tracer method indicated that the extent of atomic carbon reduction in the biomasses was less than that of atomic hydrogen and oxygen. Torrefaction also lowered the sulfur content in bamboo and oil palm over 33%. An examination of the *R*-factor and burnout of the samples suggests that more volatiles were released and a higher burnout was achieved with raw and torrefied biomasses at 250 °C than at 300 °C; however, torrefaction at 300 °C is a feasible operating condition to transform biomass into a solid fuel resembling a high-volatile bituminous coal used for blast furnaces.

© 2012 Elsevier Ltd. All rights reserved.

1. Introduction

Blast furnaces (BFs) are a crucial and the most commonly employed facility in ironmaking for the purpose of producing hot metal (Hutny et al., 1991; Gupta et al., 2008; Du et al., 2007). From the perspective of using coal as a fuel, BFs can be thought of as a counter-current reactor. That is, alternating layers of coke and ore burden are charged from the top of the furnace, whereas blast air and pulverized coal are injected from the bottom through blowpipes, injection lances and tuyeres (Du et al., 2010). By virtue of a considerable amount of coal consumed in BFs through pulverized coal injection (PCI) to provide heat for reducing iron ore (Ishii, 2000; Du and Chen, 2006), carbon dioxide emissions are inevitably encountered in the ironmaking processes. As a matter of fact, CO_2 liberated from BFs approximately account for 3.5–5% of total anthropogenic CO_2 emissions (Wang et al., 2009).

Over the last two decades, in addition to bituminous and subbituminous coals, attempts have been made to use a variety of other feedstocks, such as coal blends (Shen et al., 2009a,b; Du et al., 2010), charcoal (Machado et al., 2010), waste plastics (Ziebik and Stanek, 2001) and biomass (Chen and Wu, 2009), for injection into BFs to increase the operational flexibility of PCI. The utilization of alternatives to coal in PCI can abate the consumption of fossil fuels and, in the case of biomass, mitigate CO_2 emissions. If biomass can be used in BFs as an alternative fuel to coal, it is anticipated that CO_2 emissions from the steel industry and ironmaking can be lessened to a certain extent. However, application of biomass as an industrial fuel is limited due to its high moisture, low bulk and energy densities as well as hard grindability (Chen and Kuo, 2010).

Torrefaction has displayed numerous merits in improving the properties of biomass. Specifically, when biomass is heated in an inert or nitrogen atmosphere at 200–300 °C, moisture as well as H/C and O/C ratios of biomass will be reduced and its heating value is increased (Prins et al., 2006a,b; Almeida et al., 2010). As a result, the pretreatment is able to (1) convert a hygroscopic biomass into a hydrophobic one; (2) improve ignitability, grindability and reactivity of the biomass; and (3) make storage and handling of the torrefied biomass easier (Arias et al., 2008; Bridgeman et al., 2008; Phanphanich and Mani, 2010; Repellin et al., 2010). If the torrefied biomass is further compressed and converted into pellets, the bulky behavior of biomass can be resolved and the delivery of the biomass is more efficient. Since most of the hemicellulose in biomass can be removed by torrefaction (Rousset et al., 2009, 2011), this process renders the properties of diverse types of biomass more uniform.

In the iron and steel industries, drop tube furnaces (DTFs) have been widely utilized to evaluate combustibility and burning performance of fuels employed for PCI (Yu et al., 2007; Chen and Wu, 2009). The temperature in the chamber of a DTF is usually

---

* Corresponding author. Tel.: +886 6 2605031; fax: +886 6 2602205.
E-mail address: weihsinchen@gmail.com (W.-H. Chen).

0960-8524/$ - see front matter © 2012 Elsevier Ltd. All rights reserved.
doi:10.1016/j.biortech.2012.01.163

controlled between 1000 and 1500 °C. When pulverized fuels are transported into a DTF, the typical traveling time is in the order of 0.1 s so that the heating rate of fuel particles is usually no less than 10^4 °C s^{-1}. For this reason, the DTF is a feasible facility to simulate the combusting processes of fuel particles in BFs. A number of studies concerning biomass torrefaction have been carried out (Prins et al., 2006a,b; Arias et al., 2008; Bridgeman et al., 2008; Chen and Kuo, 2010; Rousset et al., 2011); however, research on combustibility of torrefied biomass remains insufficient, especially for evaluating burning characteristics of biomass consumed in BFs. In the present study, torrefaction and combustibility of five kinds of biomasses were investigated. Torrefaction temperatures of 250 and 300 °C were applied for 1 h to determine the impact of torrefaction on the burning behavior of the biomasses. A high-volatile bituminous coal used for PCI in BFs was also studied for comparison. The results provide useful insight into the development of solid biofuel for BFs.

2. Experimental

2.1. Reaction system

The schematic of the reaction system for testing combustibility of fuel is demonstrated in Fig. 1. Overall, the system was divided into a feeding unit, a reactor (i.e. the DTF) and a particle collection unit. In the feeding unit, two rotameters, a hopper, a screw feeder, a lance and an electric hammer were included. The rotameters were used to control the carrier gas and the secondary gas; the tested fuels were stored in the hopper. The screw feeder was utilized for controlling the feeding rate of fuel particles; the hammer was arranged to periodically knock the lance during the experiments to aid in dispersing fuel particles into the carrier gas. The DTF comprised a SiC heating element, an *R*-type thermocouple and a ceramic tube with the internal diameter of 70 mm. The heating element was controlled by a PID (proportional band integral derivative) temperature controller and a SCR (silicon controlled rectifier) power controller. The *R*-type thermocouple was mounted inside the reactor to detect the temperature of the reaction zone and the detected temperature was used as the reference of the SCR. The two ends of the reactor were sealed by high temperature o-rings. The particle collection unit was made up of a sampling probe, a cyclone and an induced suction fan. The sampling probe was enveloped by a water jacket which was filled with cooling water to protect the probe. The position of the probe was adjustable for controlling the residence time of fuel particles in the reaction zone. A cooling nitrogen stream was arranged at the entrance of the probe to prevent further reaction of the collected particles when they entered the probe. The cyclone below the sampling probe was employed to collect the residual solid particles. The induced suction fan was connected to the exit of the cyclone to keep the particles moving straightforward into the probe.

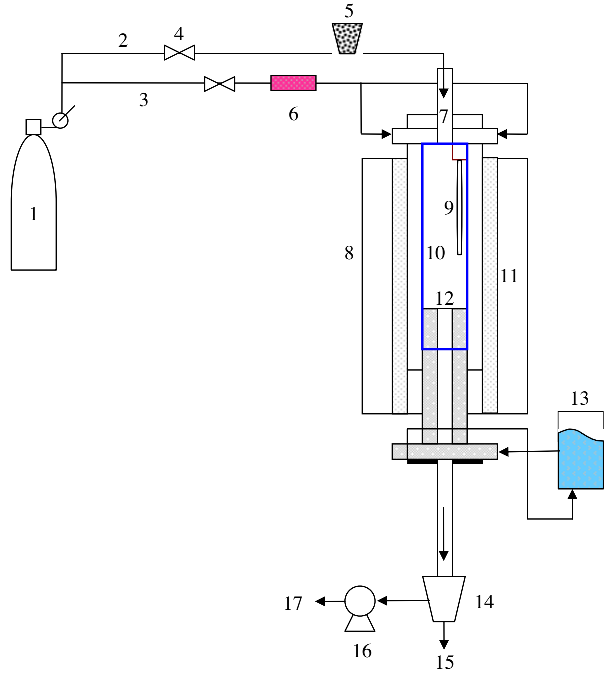

Fig. 1. Schematic of the reaction system (1) cylinder; (2) carrier gas; (3) secondary gas; (4) rotameter; (5) hopper; (6) preheater; (7) lance; (8) DTF; (9) thermocouple; (10) ceramic tube; (11) heater; (12) sampling probe; (13) cooling water; (14) cyclone; (15) residual solid particles; (16) induced suction fan; (17) exhausted gas.

2.2. Material preparation

Bamboo, oil palm, rice husk, bagasse and Madagascar almond were tested to account for the impact of torrefaction upon their burning characteristics. A high-volatile bituminous coal, which is used in China Steel Corporation (CSC) for PCI and power, was also studied for comparison. The proximate, elemental, fiber and calorific analyses of the coal and raw biomasses are tabulated in Table 1. The higher heating value (HHV) was obtained from the calorific analysis. Bamboo, oil palm and Madagascar almond were shredded by a cutting shredder to a particle size of 5–10 mesh (i.e. 2–4 mm), whereas rice husk and bagasse were not treated. The five biomasses were kept in a 75 °C oven filled with nitrogen until torrefaction was carried out. When the biomass samples were torrefied, the nitrogen flow rate was fixed at 350 mL min^{-1} (25 °C) and the torrefaction duration was 1 h. After the torrefaction was implemented, the oven was heated to 600 °C and air was blown to burn residual tars. The torrefied materials were ground into powders with a shedder followed by sieving using vibrating screens to the particle sizes of 100–200 mesh (i.e. 74–149 μm). Afterwards, the torrefied biomasses were stored in an oven filled with N_2 at 75 °C.

2.3. Experimental procedure and conditions

During the experiments, prepared fuel particles stored in the hopper were fed by a screw feeder. The particles and the carrier gas with a flow rate of 2 L min^{-1} were introduced from the top of

Table 1
Proximate, elemental, fiber and calorific analyses of the investigated coal and raw biomasses.

	Coal	Bamboo	Oil palm	Rice husk	Bagasse	Madagascar almond
Proximate analysis (wt.%)						
Moisture	13.92	5.76	7.20	8.00	7.03	10.17
VM	44.09	78.76	67.25	73.18	75.03	70.38
FC	40.47	14.40	19.03	9.27	13.61	18.62
Ash	1.52	1.08	6.52	9.55	4.33	0.83
Elemental analysis (wt.%, dry basis)						
C	63.72	48.64	44.81	43.40	46.38	47.68
H	4.40	5.64	4.10	4.33	4.68	4.31
N	0.67	0.52	2.10	0.65	0.50	0.50
S	0.10	0.03	0.24	0	0	0
O (by diff.)	29.59	44.09	42.23	42.07	44.11	46.68
Fiber analysis (wt.%)						
Hemicellulose	–	20.38	34.00	21.34	30.59	18.23
Cellulose	–	39.82	26.78	36.06	45.66	41.86
Lignin	–	12.16	16.08	21.16	19.38	16.17
Ash	–	0.36	0.55	7.96	0.88	0.18
Other	–	27.28	22.59	13.48	4.49	23.56
HHV (kcal kg^{-1})						
	5740	4530	4092	4172	4376	4139

the reactor and travelled along the centerline of the ceramic tube. The temperature of the carrier gas was 25 °C to avoid chemical reactions in the course of transporting fuel particles. To lessen agglomeration of fuel particles, the feeding rate of the particles was controlled at around 5 g h^{-1}. The secondary gas with a flow rate of 3 L min^{-1} was preheated to 350 °C followed by blowing into four metal tubes around the lance. The arrangement of the four tubes provided a more uniform velocity distribution of the gas stream due to the injection of the carrier gas from the lance. In the DTF, a reaction temperature of 1000 °C was adopted as the base experimental condition. Corresponding to the tests of *R*-factor and burnout, the carrier and secondary gases were nitrogen and air, respectively. The residual solid particles were collected by the cyclone below the sampling probe. To ensure experimental quality, the axial temperature distribution in the DTF was measured by means of a K-type thermocouple. The distribution was fairly uniform at the center of the DTF and the reaction zone was around 30 cm and the gas temperature was spatially homogeneous in the reaction zone. The reaction system was leak-tested using nitrogen before the experiments were performed. Alternatively, the burnout experiments were carried out at least twice for some tested biomasses to ascertain experimental stability and accuracy. The relative error between each run was less than 5%.

2.4. Ash tracer method, R-factor and burnout

The ash tracer method was employed to evaluate the weight loss of carbon and it is expressed as

$$\text{weight loss of carbon } (\%) = \left[1 - \frac{(C/\text{ash})_{\text{torrefied}}}{(C/\text{ash})_{\text{raw}}}\right] \times 100 \tag{1}$$

where *C* and ash denote the weight percentages of carbon and ash in a sample. The *R*-factor, which is also established based on the ash tracer method, is defined by

$$R\text{-factor} = \frac{V}{W_{\text{VM}}} \tag{2}$$

where W_{VM} means the volatile matter content (wt.%) in a fuel under dry-ash-free, and *V*, which essentially represents the volatile yield, is given by

$$V = \left(1 - \frac{\text{Ash}_{\text{fuel}}(\%\text{dry fuel})}{\text{Ash}_{\text{char}}(\%\text{dry fuel})}\right) \times 100 \tag{3}$$

In the foregoing equation, Ash_{fuel} and Ash_{char} represent the ash contents (wt.%) in the fuel (dry basis) and in the char, respectively. With regard to the index of burnout, it is expressed as

$$\text{Burnout } (\%) = \frac{\text{Ash}_{\text{uc}} - \text{Ash}_{\text{raw}}}{\text{Ash}_{\text{uc}}\left(1 - \frac{\text{Ash}_{\text{raw}}}{100}\right)} \times 100 \tag{4}$$

where Ash_{uc} and Ash_{raw} designate the ash contents in the unburned char and raw fuel, respectively.

3. Results and discussion

3.1. Influence of torrefaction on biomass

The proximate, elemental and calorific analyses of the torrefied biomasses at 250 and 300 °C are listed in Table 2. When compared to the moisture content shown in Table 1, torrefaction reduced the moisture, and the higher the torrefaction temperature, the lower the moisture content in the torrefied biomass. In the case of Madagascar almond, the moisture decreased from 10.17% to 2.55% when the biomass underwent torrefaction at 250 °C. For the coal, fixed carbon (FC) and carbon content (*C*) were much higher than those of the biomasses, whereas its volatile matter (VM) was much lower. However, once the biomasses were torrefied at 300 °C, their properties became similar to those of coal. A small amount of sulfur was presented in raw bamboo and oil palm. After torrefaction, the sulfur content decreased over 33% at least and an increase in torrefaction temperature reduced the sulfur content more (Table 2). For example, raw and torrefied oil palm at 250 and 300 °C had sulfur contents of 0.24, 0.16 and 0 wt.%, respectively.

The van Krevelen diagram of the coal and biomasses (Fig. 2) reveals a linear correlation between the atomic H/C ratio and the atomic O/C ratio because of $R^2 = 0.765$. In addition, three groups representing the raw biomasses (Group I) and the torrefied biomasses at 250 (Group II) and 300 °C (Group III) can be identified. For Group I, the O/C ratio is located at around 0.7. With regard to Group II and III, the ratios are approximately in the ranges of 0.4–0.5 and 0.2–0.3, respectively. Accordingly, increasing torrefaction temperature markedly abates both the H/C and O/C ratios. The

Table 2
Proximate, elemental and calorific analyses of torrefied biomasses.

Torrefaction temperature	Bamboo	Oil palm	Rice husk	Bagasse	Madagascar almond
250 °C					
Moisture	3.32	3.69	2.67	2.45	2.55
VM	70.20	53.76	61.88	65.18	61.51
FC	25.05	32.58	22.27	25.27	34.87
Ash	1.43	9.97	13.18	7.10	1.07
C	56.58	54.41	48.05	53.04	61.29
H	5.55	4.54	4.63	4.97	5.10
N	0.52	1.54	0.70	0.55	0.50
S	0.02	0.16	0.00	0.00	0.00
O (by diff.)	35.90	29.38	33.44	34.34	32.04
HHV (kcal kg^{-1})	5023	4927	4226	5002	5629
300 °C					
Moisture	2.97	3.21	2.39	1.96	2.50
VM	48.05	39.60	33.33	45.00	39.97
FC	47.03	43.67	41.17	41.33	55.79
Ash	1.95	13.52	23.11	11.71	1.74
C	69.56	62.90	55.47	65.59	71.71
H	4.77	3.82	3.29	4.31	4.18
N	0.12	1.70	0.50	0.28	0.21
S	0.00	0.00	0.00	0.00	0.00
O (by diff.)	23.60	18.06	17.63	18.11	22.16
HHV (kcal kg^{-1})	6515	5625	5134	5581	6373

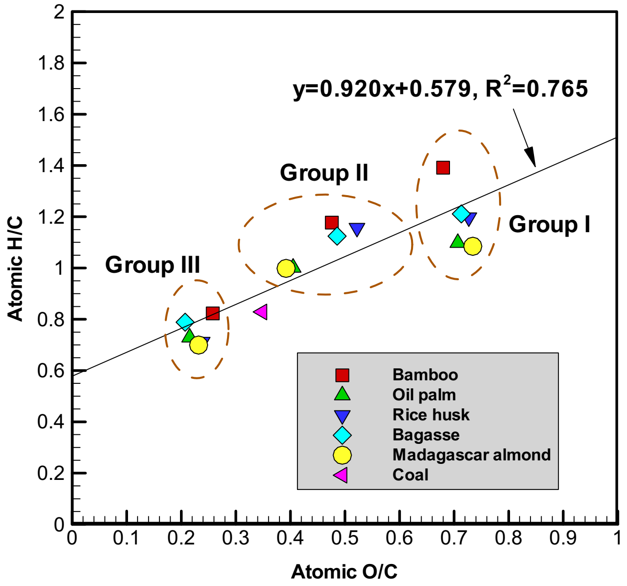

Fig. 2. Plot of atomic H/C ratio versus atomic O/C ratio of raw and torrefied biomasses and coal.

slope of the regression line is 0.92. This reflects that the influence of torrefaction on the O/C ratio exceeds the H/C ratio and this behavior is consistent with the observations of van der Stelt et al. (2011) and Rousset et al. (2011).

3.2. Calorific value and element loss

The higher heating value (HHV) ratios (enhancement factors) for raw and torrefied biomasses and coal are listed in Table 3. From a calorific point of view, Madagascar almond was the most sensitive biomass to torrefaction. Specifically, with torrefaction temperatures of 250 and 300 °C, its HHV was amplified by factors of 1.36 and 1.54, respectively. For the torrefaction temperature of 300 °C, the calorific values of the biomasses were close to that of coal, except for rice husk, which had enhancement factors of around unity. This reveals that 300 °C is a feasible operating condition to transform the biomasses into solid fuels resembling high-volatile bituminous coal.

Though torrefaction can promote the energy density of biomass, the disadvantage accompanied by the pretreatment is weight loss and therefore, reduced energy yield. To determine the weight losses of elements C, H and O in the biomasses from the two torrefactions, the ash tracer method was employed. This method assumes that ash is an inert material and conserved during torrefaction. In biomass, alkali and alkaline species, such as Na, K and Mg, are usually contained in ash in the form of Na_2O, K_2O and MgO (Yang et al., 2006; Vassilev et al., 2010; Cui et al., 2011). The boiling points of Na_2O and MgO are higher than 1950 and 3600 °C, respectively. This implies that they are hardly affected when the ash tracer method is carried out. Besides, the contents of Na_2O, K_2O and MgO in ash are usually relatively low. For example, Na_2O, K_2O and MgO in the ash of oil palm fiber were 0.2, 12.6 and 7.1 wt.%, respectively (Yang et al., 2006). Vassilev et al. (2010) pointed out that the contents of Na_2O, K_2O and MgO in the ash of rice husk were 0.16, 2.29 and 0.19 wt.%, respectively. In the ash analysis of bagasse (Cui et al., 2011), the weight percentages of Na_2O, K_2O and MgO were 1.96, 5.10 and 2.64 wt.%, respectively. These data reveal that impact due to the release of alkali and alkaline species contained in ash might be minimal. Using the ratio of carbon to ash in biomass obtained from Tables 1 and 2, the weight loss of C was evaluated with Eq. (1). The weight losses of H and O were evaluated in the same way. The profiles of weight losses of C, H and O are displayed in Fig. 3. The weight loss of C was less than 50%, regardless of what biomass was torrefied. In contrast, it was larger than 50% for H and O when the torrefaction temperature was 300 °C. It is thus recognized that the impact of torrefaction on C is relatively slight compared that on H and O. This is the reason that the H/C and O/C ratios decreased with increasing torrefaction temperature. Fig. 3 also depicts that the rice husk and bagasse were relatively active when the torrefaction temperature was 300 °C, as more C, H and O were depleted by torrefaction.

3.3. R-factor

When a pulverized coal is injected into a BF, the parameters of *R*-factor and burnout are two important indicators to evaluate the feasibility of the fuel for PCI. Physically, the *R*-factor stands for the volatile release ratio under rapid heating condition to the standardized VM test from the ASTM (Gibbins et al., 1993; Chen et al., 2007). Hence, a higher *R*-factor implies a better devolatilization extent for fuel particles traveling in a reaction zone, whereby the gas-phase combustion can be intensified. The *R*-factors of coal

Table 3
Enhancement factor of higher heating value.

Enhancement factor	Bamboo	Oil palm	Rice husk	Bagasse	Madagascar almond
HHV_{250}/HHV_{raw}	1.11	1.20	1.01	1.14	1.36
HHV_{300}/HHV_{raw}	1.44	1.37	1.23	1.28	1.54
HHV_{raw}/HHV_{coal}	0.79	0.71	0.73	0.76	0.72
HHV_{250}/HHV_{coal}	0.88	0.86	0.74	0.87	0.98
HHV_{300}/HHV_{coal}	1.14	0.98	0.89	0.97	1.11

(a) Carbon

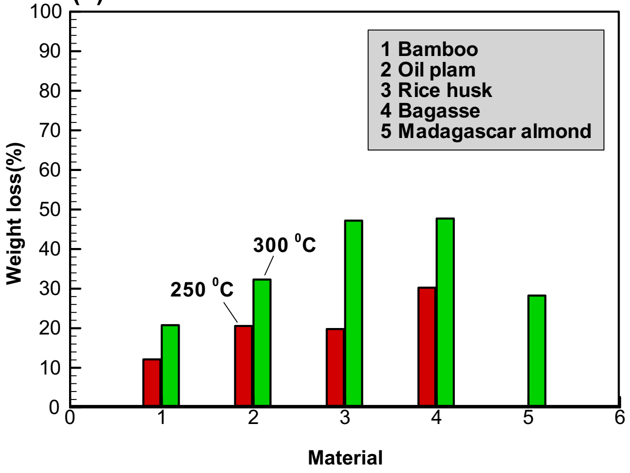

(b) Hydrogen

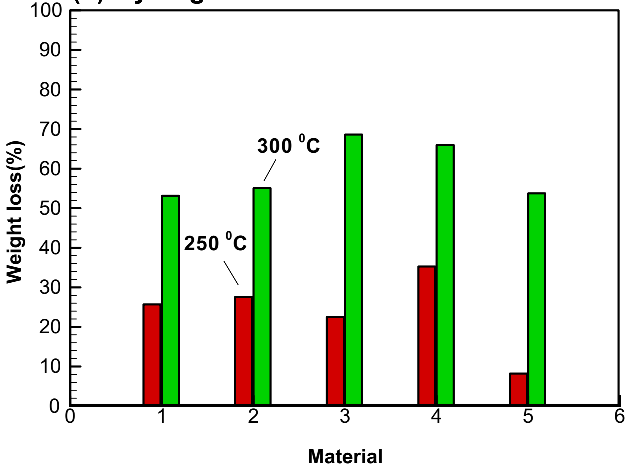

(c) Oxygen

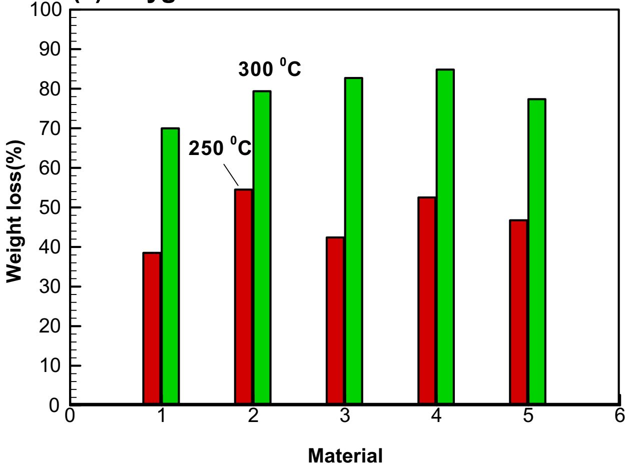

Fig. 3. Weight loss of (a) carbon, (b) hydrogen and (c) oxygen of torrefied biomasses with torrefaction temperatures of 250 and 300 °C.

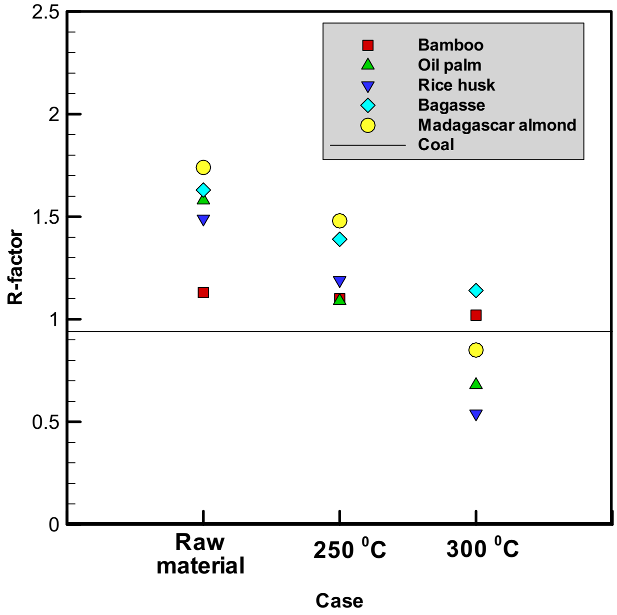

Fig. 4. *R*-factors of raw and torrefied biomasses with torrefaction temperatures of 250 and 300 °C.

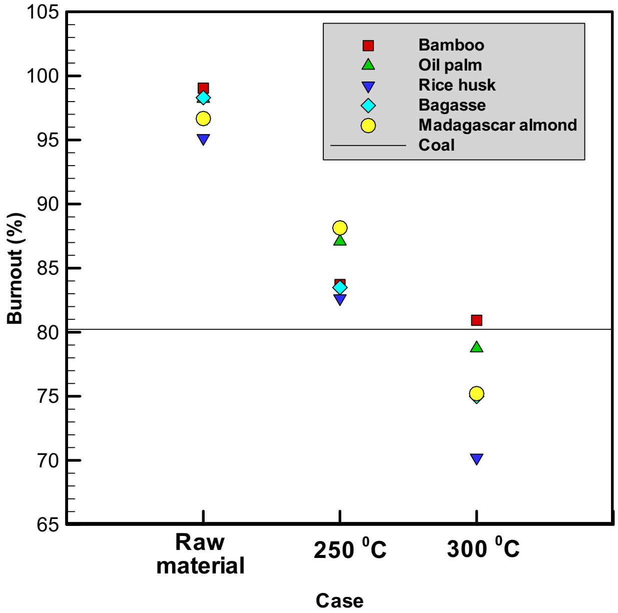

Fig. 5. Burnout of raw and torrefied biomasses with torrefaction temperatures of 250 and 300 °C.

as well as raw and torrefied biomasses after travelling in the DTF are demonstrated in Fig. 4. The profiles suggest that it was easier to release volatiles from raw and torrefied biomasses at 250 than 300 °C because the *R*-factors are larger than unity. The *R*-factors for oil palm, rice husk and Madagascar almond torrefied at 300 °C and for coal are smaller than unity, revealing that the devolatilization processes of the particles became relatively difficult. According to these observations, the particles of Group I and II are conducive to homogenous or gas-phase combustion when they are injected into a BF. Alternatively, once the powders of Group III are blown into a BF, the reactions have a trend to be dominated by the heterogeneous or solid-phase combustion.

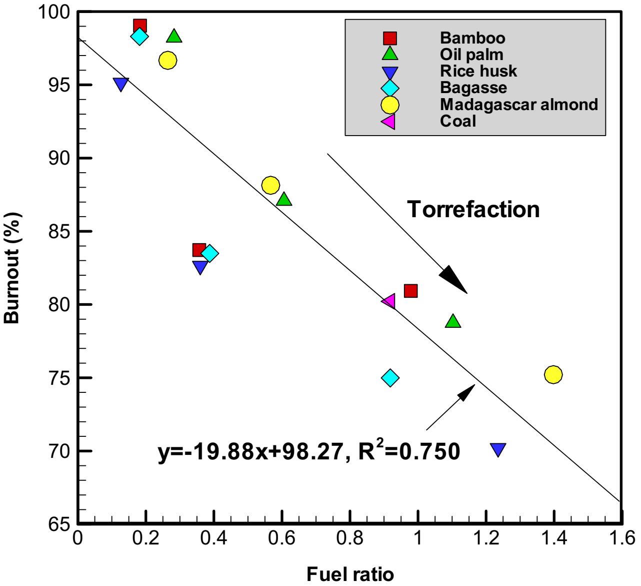

Fig. 6. Distributions of burnout versus fuel ratio of raw and torrefied biomasses as well as a coal.

3.4. Burnout

The combustion efficiency of a fuel is often measured in terms of burnout (Osório et al., 2006; Shen et al., 2009a,b). Physically, the higher the burnout, the better the combustibility of a fuel is. Fig. 5 indicates that the values of burnout of Group I were always larger than 95%, reflecting that over 95% of combustible components in the raw biomasses are consumed in the DTF. For Group II, the burnout was between 82% and 88%. A comparison with the burnout of the coal (=80.2%) suggests that the reactivity of Group I and II was better. Considering Group III, burnout (viz. 70.2–80.9) was lower than that of coal, except for bamboo. From the viewpoint of biomass applied in BFs, the residence times of Group I and II in the raceway can be shortened. In regard to Group III, on account of the fuels featured by lower burnout, the torrefied biomasses can be injected with lower velocities for complete combustion.

The burnout versus fuel ratio of the samples is demonstrated in Fig. 6. The fuel ratio is defined as the content ratio of FC to VM (Kurose et al., 2004; Du et al., 2010). The fuel ratio is in the range of 0.13–1.4. Once the biomasses underwent torrefaction, the burnout tended to decay, whereas the fuel ratio shifted rightwards in the diagram. For the biomasses in Group III, the fuel ratios were close to that of high-volatile bituminous coal; however, these values were still much lower than those of low-volatile bituminous coals since they had higher calorific values along with fuel ratios ranging from 5.5 to 6.2 (Du et al., 2010). Therefore, torrefied biomass can be used as alternative fuels to high-volatile bituminous coals rather than low-volatile ones. A linear correlation between burnout and fuel ratio is apparently exhibited, implying that the combusting behavior of biomass can be evaluated from its fuel ratio whether the biomass is torrefied or not.

4. Conclusions

Torrefaction and burning characteristics of five biomasses have been investigated and compared to a high-volatile bituminous coal. A higher torrefaction temperature intensifies the hydrophobic nature of biomass. The weight losses of H and O in biomass due to torrefaction are beyond that of C. Moreover, the sulfur content is also reduced by torrefaction. The *R*-factors of the fuels demonstrate that torrefied biomass facilitated the gas-phase or the solid-phase combustion. Overall, the torrefaction temperature of 300 °C is a feasible operating condition to transform biomass into an alternative fuel to coal consumed for blast furnaces.

References

Almeida, G., Brito, J.O., Perre, P., 2010. Alternations in energy properties of eucalyptus wood and bark subjected to torrefaction: the potential of mass loss as a synthetic indicator. Bioresour. Technol. 101, 9778–9784.

Arias, B., Pevida, C., Fermoso, J., Plaza, M.G., Rubiera, F., Pis, J.J., 2008. Influence of torrefaction on the grindability and reactivity of woody biomass. Fuel Proces. Technol. 89, 169–175.

Bridgeman, T.G., Jones, J.M., Shield, I., Williams, P.T., 2008. Torrefaction of reed canary grass, wheat straw and willow to enhance solid fuel qualities and combustion properties. Fuel 87, 844–856.

Chen, W.H., Kuo, P.C., 2010. A study on torrefaction of various biomass materials and its impact on lignocellulosic structure simulated by a thermogravimetry. Energy 35, 2580–2586.

Chen, W.H., Wu, J.S., 2009. An evaluation on rice husk and pulverized coal blends using a drop tube furnace and a thermogravimetric analyzer for application to a blast furnace. Energy 34, 1458–1466.

Chen, W.H., Du, S.W., Yang, T.H., 2007. Volatile release and particle formation characteristics of injected pulverized coal in blast furnace. Energy Convers. Manag. 48, 2025–2033.

Cui, H, Turn, S.Q., Keffer, V., Evans, D., Tran, T., Foley, M. Study on the fate of metal elements from biomass in a bench-scale fluidized bed gasifier. Fuel. doi:10.1016/j.fuel.2011.07.029.

Du, S.W., Chen, W.H., 2006. Numerical prediction and practical improvement of pulverized coal combustion in blast furnace. Int. Comm. Heat Mass Transfer 33, 327–334.

Du, S.W., Chen, W.H., Lucas, J., 2007. Performances of pulverized coal injection in blowpipe and tuyere at various operational conditions. Energy Convers. Manag. 48, 2069–2076.

Du, S.W., Chen, W.H., Lucas, J.A., 2010. Pulverized coal burnout in blast furnace simulated by a drop tube furnace. Energy 35, 576–581.

Gibbins, J.R., Man, C.K., Pendlebury, K.J., 1993. Determination of rapid heating volatile matter contents as a routine test. Combust. Sci. Technol. 93, 349–361.

Gupta, S., French, D., Sakurovs, R., Grigore, M., Sun, H., Cham, T., Hilding, T., Hallin, M., Lindblom, B., Sahajwalla, V., 2008. Minerals and iron-making reactions in blast furnaces. Prog. Energ. Combust. Sci. 34, 155–197.

Hutny, W.P., Lee, G.K., Price, J.T., 1991. Fundamentals of coal combustion during injection into a blast furnace. Prog. Energ. Combust. Sci. 17, 373–395.

Ishii, K., 2000. Advanced Pulverised Coal Injection Technology and Blast Furnace Operation. Pergamon Publishers, Oxford.

Kurose, R., Ikeda, M., Makino, H., Kimoto, M., Miyazaki, T., 2004. Pulverized coal combustion characteristics of high-fuel-ratio coals. Fuel 83, 1777–1785.

Machado, J.G.M.S., Osorio, E., Vilela, A.C.F., Babich, A., Senk, D., Gudenau, H.W., 2010. Reactivity and conversion behaviour of Brazilian and imported coals, charcoal and blends in view of their injection into blast furnaces. Steel Res. Int. 81, 9–16.

Osório, E., Gomes, M.D.I., Vilela, A.C.F., Kalkreuth, W., de Almeida, M.A.A., Borrego, A.G., Alvarez, D., 2006. Evaluation of petrology and reactivity of coal blends for use in pulverized coal injection (PCI). Int. J. Coal Geol. 68, 14–29.

Phanphanich, M., Mani, S., 2010. Impact of torrefaction on the grindability and fuel characteristics of forest biomass. Bioresour. Technol. 102, 1246–1253.

Prins, M.J., Ptasinski, K.J., Janssen, F.J.J.G., 2006a. Torrefaction of wood. Part 1. Weight loss kinetics. J. Anal. Appl. Pyrol. 77, 28–34.

Prins, M.J., Ptasinski, K.J., Janssen, F.J.J.G., 2006b. Torrefaction of wood. Part 2. Analysis of products. J. Anal. Appl. Pyrol. 77, 35–40.

Repellin, V., Govin, A., Rolland, M., Guyonnet, R., 2010. Energy requirement for fine grinding of torrefied wood. Biomass Bioenerg. 34, 923–930.

Rousset, P., Lapierre, C., Perre, P., Quirino, W., 2009. Effect of severe thermal treatment on spuce and beech wood lignins. Ann. Forest Sci. 66, 110–118.

Rousset, P., Aguiar, C., Labbe, N., Commandre, J.M., 2011. Enhancing the combustible properties of bamboo by torrefaction. Bioresour. Technol. 102, 8225–8231.

Shen, Y.S., Guo, B.Y., Yu, A.B., Zulli, P., 2009a. A three-dimensional numerical study of the combustion of coal blends in blast furnace. Fuel 88, 255–263.

Shen, Y.S., Guo, B.Y., Yu, A.B., Zulli, P., 2009b. Model study of the effects of coal properties and blast conditions on pulverized coal combustion. ISIJ Int. 49, 819–826.

van der Stelt, M.J.C., Gerhauser, H., Kiel, J.H.A., Ptasinski, K.J., 2011. Biomass upgrading torrefaction for the production of biofuels: a review. Biomass Bioenerg. 35, 3748–3762.

Vassilev, S.V., Baxter, D., Andersen, L.K., Vassileva, C.G., 2010. An overview of the chemical composition of biomass. Fuel 89, 913–933.

Wang, C., Ryman, C., Dahl, J., 2009. Potential CO_2 emission reduction for BF-BOF steelmaking based on optimised use of ferrous burden materials. Int. J. Greenhouse Gas Control 3, 29–38.

Yang, H., Yan, R., Chen, H., Zheng, C., Lee, D.H., Liang, D.T., 2006. Influence of mineral matter on pyrolysis of palm oil wastes. Combust. Flame 146, 605–611.

Yu, J., Lucas, J.A., Wall, T.F., 2007. Formation of the structure of chars during devolatilization of pulverized coal and its thermoproperties: a review. Prog. Energ. Combust. Sci. 33, 135–170.

Ziebik, A., Stanek, W., 2001. Forecasting of the energy effects of injecting plastic wastes into the blast furnace in comparison with other auxiliary fuels. Energy 26, 1159–1173.